Journal of Ocean Engineering and Science 11 (2026) 1–12

Contents lists available at ScienceDirect

Journal of Ocean Engineering and Science

journal homepage: www.elsevier.com/locate/joes

Research paper

Phase plane bifurcation analysis of water wave dynamics in the simplified modified Camassa–Holm model with friction and wind effects

Md. Ekramul Islam [a], Md. Abde Mannaf [a,b], Mst. Tania Khatun [a], Md. Azizur Rahman [a], M. Ali Akbar [c], Udoy S. Basak [a,d,e,*]

[a] Department of Mathematics, Pabna University of Science and Technology (PUST), Bangladesh
[b] Department of Computer Science and Engineering, Northern University Bangladesh, Bangladesh
[c] Department of Applied Mathematics, University of Rajshahi, Bangladesh
[d] Max Planck Institute of Animal Behavior, Universitätstr. 10, 78464, Konstanz, Germany
[e] Department of Collective Behavior, University of Konstanz, Universitätstr. 10, 78464, Konstanz, Germany

ARTICLE INFO

Keywords:
Bifurcation analysis
Phase portrait
Hamiltonian equation
The SMCH model
Solitary wave

ABSTRACT

The simplified modified Camassa–Holm equation plays a pivotal role in modeling nonlinear wave dynamics across diverse fields, including optical fibers, biological transport, plasma physics, and shallow water flows. Its unique mathematical structure captures essential features of wave-breaking phenomena, peakon interactions, and dispersive effects that are crucial for understanding real-world wave behavior. Motivated by the need to predict extreme wave events and design efficient wave energy systems, this study investigates how external forces such as friction and wind influence wave dynamics. We explore rich dynamical transitions through a detailed bifurcation analysis. Our systematic investigation reveals critical thresholds in parameter space where small changes in forcing conditions lead to dramatic transformations in wave behavior. We identify key equilibrium states, nodes, foci, centres, and saddle points, that govern the system's response, leading to the discovery of novel wave solutions, including kink-like waves, periodic structures, and breather-like solitons. These soliton shapes have potential applications in coastal protection, energy harvesting from waves, and signal modulation in nonlinear optical systems, highlighting their practical significance. These solutions are rigorously validated through numerical simulations and stability analysis, confirming their physical relevance across different parameter regimes. The solutions are derived in exact analytical forms using hyperbolic and trigonometric functions, revealing how parameter variations trigger qualitative shifts in wave patterns. Specifically, we demonstrate how the wind parameter α controls wave amplification while the friction parameter β governs energy dissipation, providing a complete picture of their competing effects on wave evolution. Our findings deepen the theoretical understanding of nonlinear waves while offering practical insights for coastal engineering, climate modeling, signal transmission, and wave energy systems. By explicitly linking solution families to potential engineering applications, this study provides a framework for designing devices that exploit specific soliton structures to achieve targeted wave control and energy efficiency. The methodology developed here can be readily extended to other nonlinear dispersive systems, opening new avenues for investigating wave-structure interactions in various physical contexts.

1. Introduction

Recent research has focused extensively on the applications of nonlinear evolution equations (NLEEs) across various scientific disciplines. Nonlinear partial differential equations (NLPDEs) have become crucial tools in understanding phenomena in quantum mechanics, plasma physics, electromagnetism, fluid dynamics, solid-state physics, optical fibers, and shallow water waves [1–5]. Finding analytical solutions to NLEEs holds immense potential for comprehending the intricacies of natural phenomena. These solutions provide valuable information about system behavior, enabling researchers to understand how different parameters and factors interact within the system [6,7]. Additionally, analytical solutions can simplify complex systems, leading to approximations that aid in their design and optimization. Moreover, such solutions enhance our understanding of nonlinear systems and

* Corresponding author at: Department of Mathematics, Pabna University of Science and Technology (PUST), Bangladesh.
E-mail address: udoy@pust.ac.bd (U.S. Basak).

https://doi.org/10.1016/j.joes.2025.08.008
Received 25 November 2024; Received in revised form 21 August 2025; Accepted 22 August 2025
Available online 16 September 2025

foster the development of innovative mathematical tools. While powerful techniques like computer algebra systems (e.g., Matlab, Maple, Mathematica) have been employed to find accurate soliton solutions, it is important to acknowledge the limitations in precisely controlling all model equations. This requires careful application of control or intervention methods to obtain reliable results.

Analytical methods have also been effectively used to study nonlinear wave phenomena. Recent works have reported cross-kink and solitary wave solutions in nonlinear vibration and dispersive systems [8], as well as multiple rogue wave solutions for variable-coefficient Kadomtsev–Petviashvili equations [9]. Additionally, periodic wave solutions with stability analysis have been derived for the (3+1)-dimensional potential-YTSF equation arising in fluid mechanics [10], further advancing the understanding of wave dynamics.

To address these limitations, mathematicians and physicists have devised numerous novel methods, including the MSE method [11,12], the sine-cosine method [13], Hirota's bilinear method [14–19], the tanh-function expansion method and its modifications [20,21], the new modified (G'/G)-expansion scheme [22], the unified method [23], the Kudryashov method [24], the Exp-function method [25], the bilinear neural network method [26], the binary Darboux transformation [27], the extended homogeneous balance method [28], the generalized Riccati equation mapping approach [29], the $\exp(-\phi(\eta))$-expansion method [30], the transformed rational function method [31], the Lax pair technique [32], and many others [33–42].

Understanding the dynamics of wave patterns in inland and coastal waters is essential for predicting surface wave behavior. These natural processes can greatly affect coastal regions and maritime infrastructure, highlighting the need for thorough study within ocean engineering. In recent years, research in ocean engineering and science has made significant progress in this area. An important advancement is the development of the Camassa–Holm (CH) equation, introduced in 1993 by Camassa and Holm [43]. Originally formulated to model shallow water waves, the CH equation is notable for its unique integrable bi-Hamiltonian structure. This foundational work has since inspired numerous extensions and adaptations [44–46], deepening our understanding of wave dynamics. Such developments provide essential tools for assessing and predicting wave behavior, ultimately enhancing marine infrastructure design, coastal management, and safety measures against wave-related risks.

Irshad et al. [47] extended the Camassa–Holm (CH) equation by proposing a simplified, modified version. This modification enhances the equation's analytical tractability and numerical solvability, making it a valuable tool for studying wave propagation and fluid dynamics. The Simplified Modified Camassa–Holm (SMCH) equation offers new avenues for exploring nonlinear wave phenomena and takes the following form [48]:

$$V_t + 2\alpha V_x - V_{xxt} + \beta V^2 V_x = 0, \quad \beta > 0. \tag{1.1}$$

Here, $V(x,t)$ denotes the wave profile (i.e., the fluid height) at a specific horizontal position x and time t, with α and β serving as parameters that affect the wave dynamics.

The SMCH equation has been studied through several analytical techniques, including the exp-function method [47], He's semi-inverse method [49], the generalized (G'/G)-expansion method [50], the improved (G'/G)-expansion method [51], the $\exp(-\phi(\eta))$-expansion method [52], and others [53,54]. A notable gap in the existing literature is the absence of research applying bifurcation analysis — an effective method for examining nonlinear partial differential equations (NLPDEs) — to investigate exact solutions of the SMCH equation. This study addresses this gap by employing a novel approach — bifurcation analysis — to explore the impact of free parameters on the wave profile within the SMCH model. Our investigation utilizes phase portrait analysis to determine the stability of equilibrium points within the system, specifically saddle and center points. This method provides a fresh perspective on how changes in essential parameters, like wave height and friction, influence the properties of waves described by the SMCH equation. The results of this study lay the foundation for future research opportunities. By showcasing the potential of bifurcation analysis for the SMCH equation, this work opens the door to applying this technique to other mathematical models that represent real-world phenomena.

In contrast to earlier studies that mainly focused on idealized forms of the SMCH equation, our work incorporates friction and wind effects, thereby extending the model toward more realistic wave dynamics in natural environments such as wind-driven shallow water flows and dissipative coastal systems. While many previous studies have obtained soliton and solitary wave solutions of the SMCH equation and related nonlinear wave models using various analytical methods, they generally neglected the role of dissipation and external forcing, which are crucial in practical fluid systems. Moreover, despite the rich literature on exact solutions of nonlinear evolution equations, bifurcation analysis has rarely been applied to the SMCH framework. This study fills that gap by employing a bifurcation-based approach to explore how friction and wind effects influence equilibrium structures, stability, and soliton dynamics. Thus, the novelty of our work lies in both the enriched physical formulation of the SMCH model and the methodological innovation of applying bifurcation analysis, which together provide new insights into how external forcing and dissipation reshape nonlinear wave behavior.

The paper is structured as follows: Section 2 introduces the fundamentals of the SMCH model and the wave transformation technique used to simplify and analyze the system under study. Section 3 conducts a phase portrait analysis of the SMCH model and presents phase portraits along with their physical interpretations. Section 4 focuses on the analysis of solitary and traveling waves in the SMCH model using the energy function. Section 5 compares our solutions with previously published results. Section 6 discusses the novelty of our findings and outlines potential future research directions for the SMCH model. Finally, Section 7 summarizes the main results and concludes the paper.

2. The SMCH model

The SMCH equation, which governs the dynamics of longitudinal wave propagation in the medium, is expressed as follows [55]:

$$V_t + 2\alpha V_x - V_{xxt} + \beta V^2 V_x = 0. \tag{2.1}$$

To investigate Eq. (2.1), we implement the proposed method using the wave transformation as follows:

$$V(x,t) = V(\xi), \quad \xi = x - \omega t. \tag{2.2}$$

Substituting Eq. (2.2) into Eq. (2.1) yields the nonlinear model:

$$-\omega V' + 2\alpha V' + \omega V''' + \beta V^2 V' = 0, \tag{2.3}$$

and integrating equation (2.3),

$$\omega V - 2\alpha V - \omega V'' - \frac{\beta}{3} V^3 = 0. \tag{2.4}$$

Here, the integration constant is assumed to be zero.

3. Phase portrait analysis of the SMCH model

Modifying system parameters can lead to significant changes in its behavior, including the creation or removal of fixed points and shifts in stability, known as bifurcations. These bifurcations represent points where the system undergoes fundamental changes in its dynamics. The specific parameter values at which these changes occur are called bifurcation points. Understanding bifurcations is essential for studying system transitions as parameters vary. Additionally, analyzing the evolution of orbits in the phase plane offers valuable insights into the system's dynamics, allowing for predictions about future behavior. This

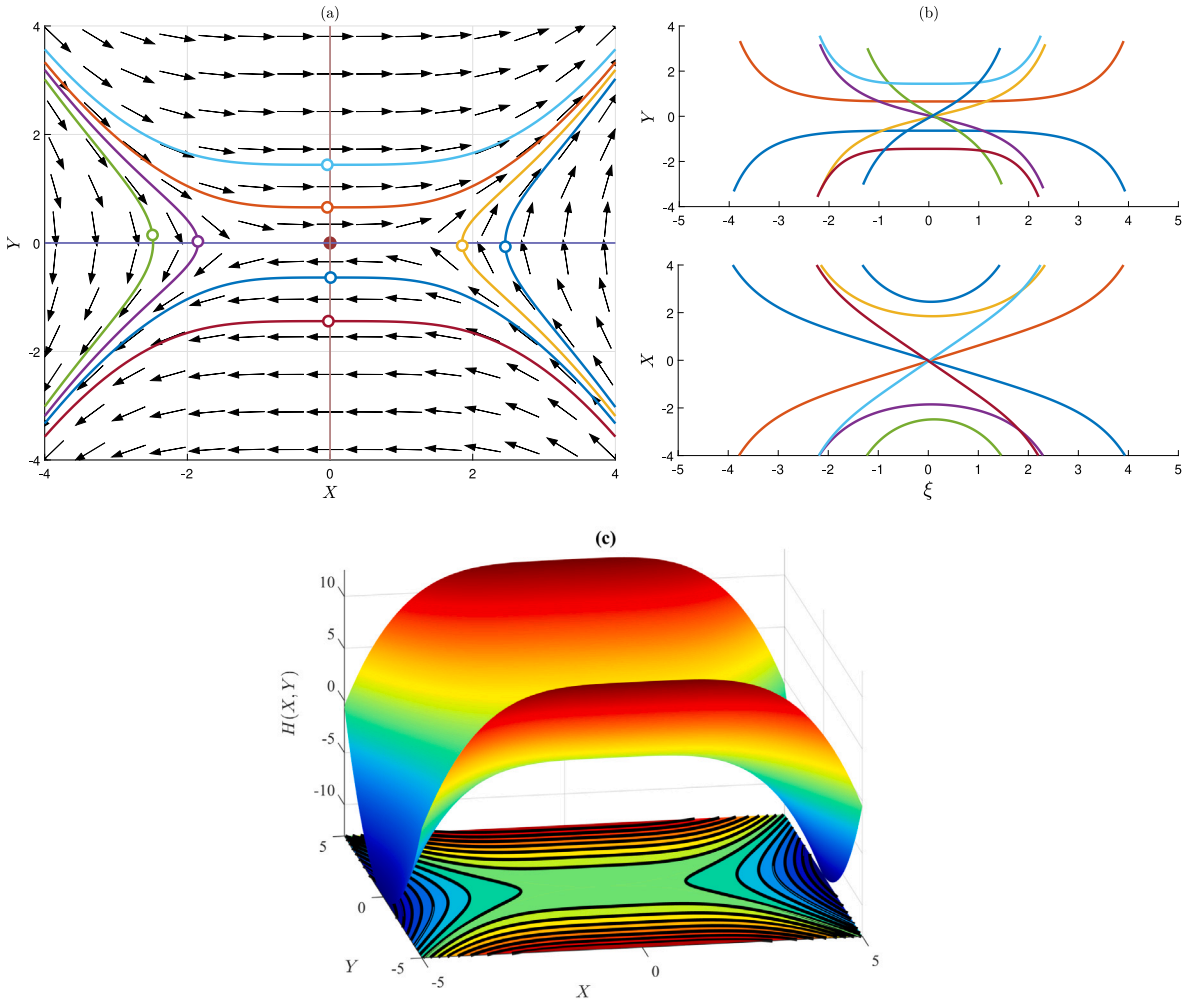

Fig. 1. The phase diagram of the two-dimensional system (3.1) is generated using the parameter values $2\alpha = \omega$ with $(\alpha = 2, \beta = 1, \omega = 4)$. Fig. 1(a) displays the trajectories followed by the system, highlighting isoclines and nullclines. In Fig. 1(b), the solutions corresponding to these trajectories are depicted, represented in relation to the wave variable ξ. Fig. 1(c) showcases the Hamiltonian plot of Eq. (3.2).

section examines the relationship between the phase diagram and its solutions in the context of the SMCH equation.

To continue using the approach in Ref. [56,57], we can express Eq. (2.4) as a system of planar dynamics by selecting $V = X$ and $V' = Y$, thus reformulating the equation as follows:

$$\begin{cases} X' = Y = f(X,Y) \\ Y' = X - \frac{2\alpha}{\omega}X + \frac{\beta}{3\omega}X^3 = g(X,Y). \end{cases} \tag{3.1}$$

The Hamiltonian function for the planar Hamiltonian system given by Eq. (3.1) is

$$H(X,Y) = \frac{Y^2}{2} + \left(\frac{\alpha}{\omega} - \frac{1}{2}\right)X^2 - \frac{\beta}{12\omega}X^4. \tag{3.2}$$

The system exhibits three equilibrium points, which are $E_0^* : (X^*, Y^*) = (0,\ 0)$, $E_1^* : (X^*, Y^*) = \left(\sqrt{\frac{6\alpha-3\omega}{\beta}},\ 0\right)$ and $E_2^* : (X^*, Y^*) = \left(-\sqrt{\frac{6\alpha-3\omega}{\beta}},\ 0\right)$. The linearization of the system described by Eq. (3.1) at the points $E_i^*(i = 0, 1, 2)$ leads to the variational equation $\Delta x' = J\Delta x$, where $x = (X, Y)^T, \Delta x = x - x^*$, and J is the Jacobian matrix, which has the following form:

$$J(X,Y) = \frac{\partial(f,g)}{\partial(X,Y)} = \begin{pmatrix} \frac{\partial f}{\partial X} & \frac{\partial f}{\partial Y} \\ \frac{\partial g}{\partial X} & \frac{\partial g}{\partial Y} \end{pmatrix}_{|(X^*,Y^*)} = \begin{pmatrix} 0 & 1 \\ 1 - \frac{2\alpha}{\omega} + \frac{\beta}{\omega}X^2 & 0 \end{pmatrix}. \tag{3.3}$$

The eigenvalues of J are given by $|J - \lambda I| = 0$ which implies,

$$\lambda^2 - tr(J)\lambda + |J| = 0, \tag{3.4}$$

where $tr(J) = 0$ and $|J| = \frac{2\alpha}{\omega} - \frac{\beta}{\omega}X^2 - 1$.

Case 01. Stability at $x^* = (0,0)^T$: In this scenario, the characteristic roots are $\lambda = \frac{\pm\sqrt{D}}{2}$, where $D = 4\left(1 - \frac{2\alpha}{\omega}\right) = 4\left(\frac{\omega-2\alpha}{\omega}\right)$. Here, the following cases arise:

(a) When $\omega = 2\alpha$, $\omega \neq 0$ implies $D = 0$. Here, the eigenvalues of the system have no imaginary parts and are equal to zero; therefore, the system is considered unstable. This scenario can be seen as a simple example of a complex eigenvalue with a zero component. The phase diagram of the two-dimensional system (3.1) is plotted with the parameter values $\alpha = 2, \omega = 4, \beta = 1$. Fig. 1(a) illustrates the paths followed by the system, showcasing isoclines and nullclines. In Fig. 1(b), the solutions corresponding to these trajectories are presented, expressed with respect to the wave variable ξ. Finally, Fig. 1(c) represents the Hamiltonian plot of (3.2).

(b) When $\omega - 2\alpha < 0$, $\omega \neq 0$ then the following cases arise:

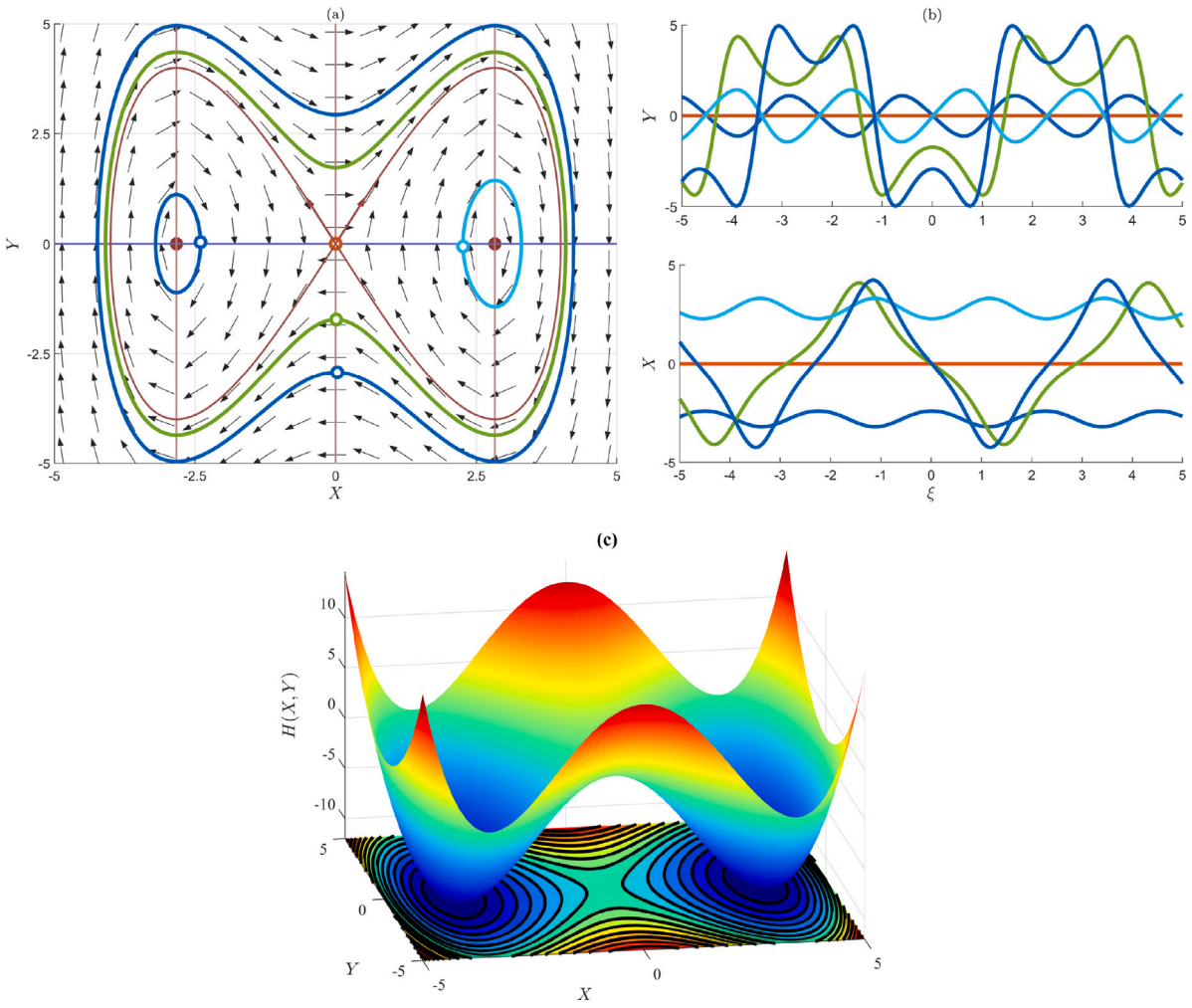

Fig. 2. The phase diagram of the two-dimensional system (3.1) is plotted using the parameter values where $\omega - 2\alpha < 0$ and $\omega < 0$, specifically $(\alpha = 3, \beta = 2, \omega = -2)$. Fig. 2(a) showcases the trajectories followed by the system, highlighting isoclines and nullclines. In Fig. 2(b), the solutions corresponding to these trajectories are displayed, expressed in relation to the wave variable ξ. Additionally, Fig. 2(c) presents the Hamiltonian plot of Eq. (3.2).

i. When $\omega < 0$, the eigenvalues

$$\lambda_1 = \sqrt{\frac{\omega - 2\alpha}{\omega}} \quad \text{and} \quad \lambda_2 = -\sqrt{\frac{\omega - 2\alpha}{\omega}}$$

are real and have opposite signs. This indicates that the equilibrium point $x^* = (0,0)^T$ behaves as an unstable saddle point, as illustrated in Figs. 2–3.

ii. If $\omega > 0$, the eigenvalues

$$\lambda_1 = i\sqrt{1 - \frac{2\alpha}{\omega}}, \quad \lambda_2 = -i\sqrt{1 - \frac{2\alpha}{\omega}}$$

are purely imaginary and complex conjugates, which means the equilibrium point $x^* = (0,0)^T$ is a stable center, as shown in Fig. 4.

(c) When $\omega - 2\alpha > 0$, $\omega \neq 0$ then the following cases arise as follows:

i. When $\omega < 0$, the eigenvalues

$$\lambda_1 = i\sqrt{1 - \frac{2\alpha}{\omega}} \quad \text{and} \quad \lambda_2 = -i\sqrt{1 - \frac{2\alpha}{\omega}}$$

are purely imaginary complex conjugates and have opposite signs. This implies that the equilibrium point $x^* = (0,0)^T$ is a stable center, as shown in Fig. 5.

ii. For $\omega > 0$, the eigenvalues

$$\lambda_1 = \sqrt{\frac{\omega - 2\alpha}{\omega}} \quad \text{and} \quad \lambda_2 = -\sqrt{\frac{\omega - 2\alpha}{\omega}}$$

are real and have opposite signs. This implies that the equilibrium point $x^* = (0,0)^T$ is an unstable saddle point, as demonstrated in Figs. 6 and 7.

Case 02. Stability at $x^* = \left(\sqrt{\frac{6\alpha - 3\omega}{\beta}}, 0\right)^T$: for this case $\beta > 0$ and the characteristic roots are $\lambda = \pm\sqrt{\frac{2(2\alpha - \omega)}{\omega}}$.

(a) If $\omega = 2\alpha$ and $\beta, \omega \neq 0$ then it is similar to the case 01 (a)
(b) If $2\alpha - \omega > 0$ then it represents case 01(b)
(c) If $2\alpha - \omega < 0$ then it corresponds to the case 01(c)

Case 03. Stability at $x^* = \left(-\sqrt{\frac{6\alpha - 3\omega}{\beta}}, 0\right)^T$: In this case, the characteristic roots are the same as those in Case 2. As a result, the nature of the eigenvalues is also identical to that of Case 1, since the behavior in Case 2 mirrors that of Case 1. Therefore,

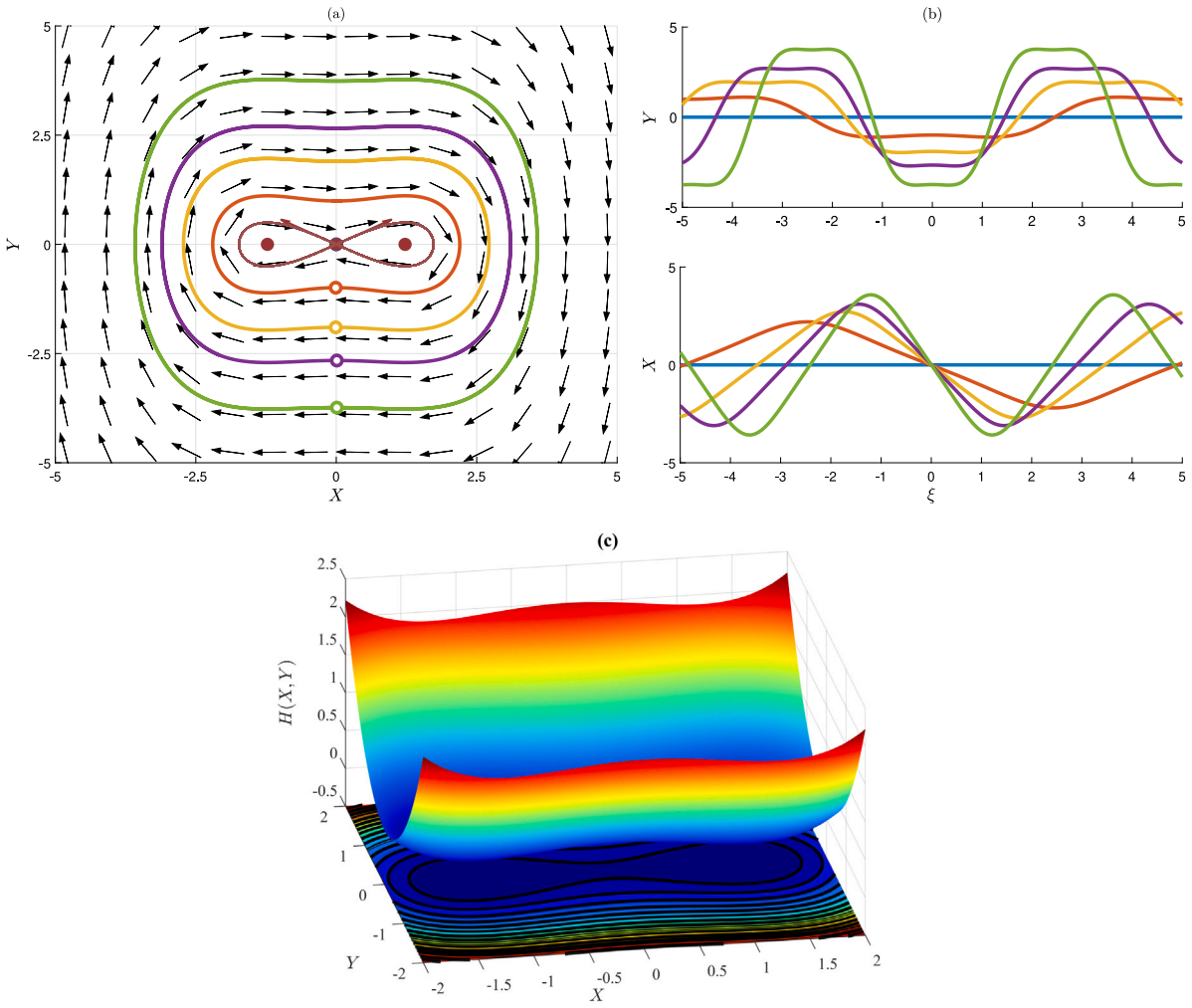

Fig. 3. The phase diagram of the system (3.1) is plotted with the parameter values $\omega - 2\alpha < 0, \omega < 0$ for $(\alpha = -1, \beta = 2, \omega = -3)$. Fig. 3(a) illustrates the paths followed by the system, showcasing isoclines and nullclines. In Fig. 3(b), the solutions corresponding to these trajectories are presented, expressed with regard to the wave variable ξ. Fig. 3(c) shows the Hamiltonian plot of Eq. (3.2).

the stability of the equilibrium point $x^* = \left(-\sqrt{\frac{6\alpha-3\omega}{\beta}}, 0\right)^T$ will not be discussed further here.

4. Analysis of solitary and traveling waves in the SMCH model

Let us consider a stochastic model with a continuous solution represented by $V(\xi)$, where $\xi \in \mathbb{R}$. If the following condition is satisfied:

$$\lim_{\xi \to -\infty} V(\xi) = \lim_{\xi \to \infty} V(\xi),$$

then the solution $V(\xi)$ corresponds to a solitary wave.

At the equilibrium points E_i (where $i = 0, 1, 2$), the energy levels are given by:

$$h_{E_0} = H(0, 0) = 0, \tag{4.1}$$

$$h_{E_1} = H\left(\sqrt{\frac{3(2\alpha - \omega)}{\beta}}, 0\right) = \frac{3\,(2\,\alpha - \omega)^2}{4\,\beta\,\omega}, \tag{4.2}$$

$$h_{E_2} = H\left(-\sqrt{\frac{3(2\alpha - \omega)}{\beta}}, 0\right) = \frac{3\,(2\,\alpha - \omega)^2}{4\,\beta\,\omega}, \tag{4.3}$$

respectively.

Using Eqs. (3.1) and (4.1) with $V = X$ and $V' = Y$, we obtained solution functions for h_{E_0} as

$$V_{3_{11}} = \pm \frac{\sqrt{6}\sqrt{\beta\left(\tan\left(\frac{\xi\sqrt{2\alpha-\omega}}{\sqrt{\omega}}\right)^2 + 1\right)(2\alpha - \omega)}}{\beta}, \tag{4.4}$$

where $\xi = x - \omega t$.

Also, using Eqs. (3.1) and (4.2) or (4.3) with $V = X$ and $V' = Y$, we obtained solution functions for h_{E_1} or h_{E_2} as

$$V_{3_{12}} = \pm \frac{\sqrt{3}\,\tanh\left(\frac{\sqrt{2}\,\xi\,\sqrt{2\alpha-\omega}}{2\sqrt{\omega}}\right)\sqrt{2\alpha - \omega}}{\sqrt{\beta}}, \tag{4.5}$$

where $\xi = x - \omega t$.

Now, we discuss the physical interpretation of the solutions given by Eqs. (4.4) and (4.5) as follows: The solution function (4.4) exhibits unequal periodic waves for different values of the parameters ω, α, and β. Figs. 8(a)–8(c) illustrate the effect of the parameter α when the velocity is very small, $\omega = 0.1$. Increasing the velocity to $\omega = 0.5$, Figs. 8(d)–8(f) show the influence of α. Furthermore, with velocity $\omega = 0.9$, the same solution demonstrates the wave behavior shown in Figs. 8(g)–8(i).

On the other hand, the soliton solution (4.5) represents kink-shaped solitons and symmetric waves for different values of the free parameters

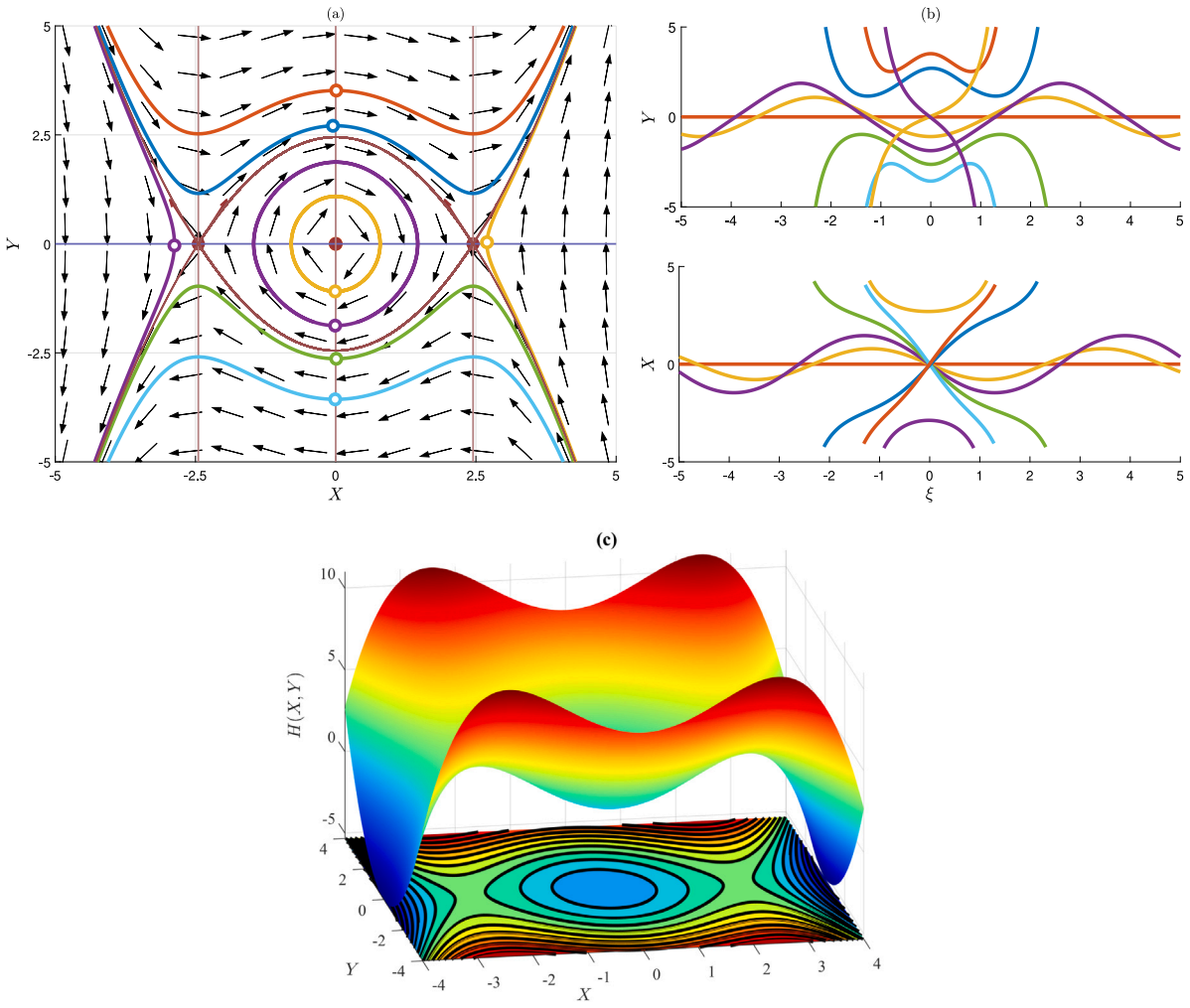

Fig. 4. The phase diagram of the two-dimensional system (3.1) is plotted with the parameter values $\omega - 2\alpha\langle 0, \omega\rangle 0$ for $(\alpha = 3, \beta = 2, \omega = 2)$. Fig. 4(a) illustrates the paths followed by the system, showcasing isoclines and nullclines. In Fig. 4(b), the solutions corresponding to these trajectories are presented, expressed in terms of the wave variable ξ. Fig. 4(c) shows the Hamiltonian plot of Eq. (3.2).

ω, α, and β. The nature of the wave profile for the above-mentioned parameter values is illustrated in Figs. 9(a)–(i).

5. Comparison

Over the past decade, numerous researchers have investigated the SMCH equation using various techniques, yielding several distinct analytic solutions. For example, the $\exp(-\phi)$-expansion method was employed by Ali et al. [52], the modified simple equation (MSE) method by Islam et al. [54], the new auxiliary equation (NAE) method by Islam et al. [58], and the improved Bernoulli sub-equation function (IBSEF) method by Mannaf et al. [48] have all produced multiple solutions for the SMCH equation.

We compare our solutions with those established by Mannaf et al. [48]. Notably, in our previous work [48], we obtained only hyperbolic-type solutions, whereas in the present study, both hyperbolic and trigonometric solutions are derived. Table 1 provides a comparison between our current solutions and the previous results.

6. Novel contributions and future scope

By applying the Improved Bernoulli Sub-Equation Function (IBSEF) method to the SMCH model, Mannaf et al. [48] previously derived a single class of classical hyperbolic solutions. In contrast, our study has not only reproduced those results through various parameter combinations but has also yielded a wider range of solutions, including trigonometric, kink-shaped, and symmetric waveforms, with improved quality and resolution.

Whereas Mannaf et al. obtained kink, bright, and dark-type solitons using their specific technique, we achieved a more diverse family of solutions by leveraging the energy function. These include unequal periodic waves, kink-type solitons, and symmetric waveforms—broadening the applicability and interpretability of the SMCH model in representing real-world wave dynamics.

A key novelty of this work lies in the incorporation of bifurcation analysis and phase portraits. This approach allows us to pinpoint critical transitions in system dynamics, marking a significant advancement not previously applied to the SMCH model. Our bifurcation-based exploration of the wind influence parameter (α) and the friction damping parameter (β) offers fresh insights into their roles in stabilizing or destabilizing wave profiles. Furthermore, the Hamiltonian structure is used to classify and predict stable versus unstable equilibria and to understand how these equilibria evolve over time.

This research highlights the strength of exact optical soliton solutions and the role of energy-based analysis in unveiling complex nonlinear behaviors. Future work may extend this approach to include the variational wave method or examine the emergence of chaotic dynamics—both of which offer promising directions for deepening theoretical understanding and supporting practical applications in physics, engineering, and environmental sciences.

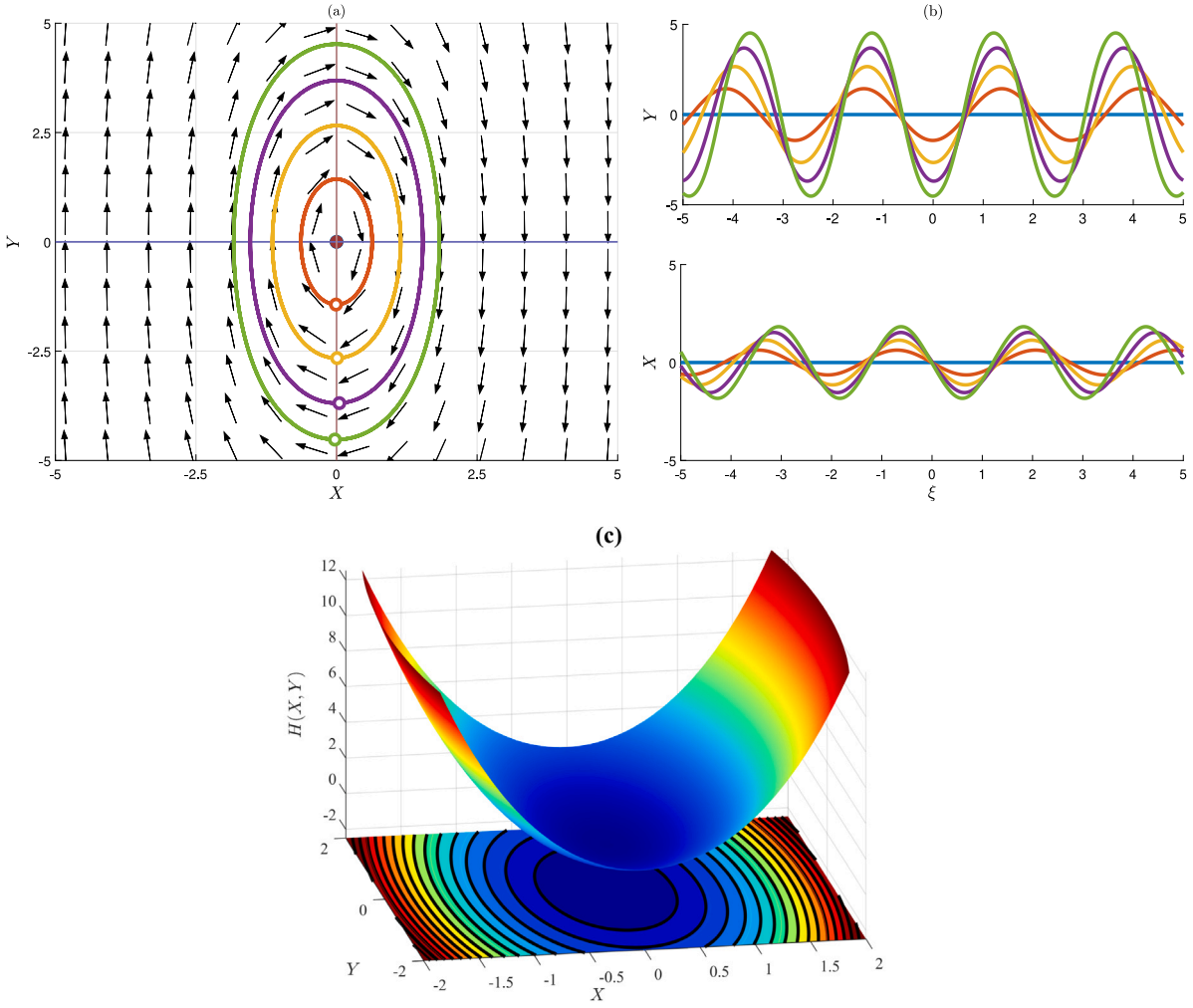

Fig. 5. The phase portrait of the two-dimensional system (3.1) is plotted with the parameter values $\omega - 2\alpha > 0, \omega < 0$ ($\alpha = -3, \beta = 2, \omega = -1$). Fig. 5(a) illustrates the paths followed by the system, showcasing isoclines and nullclines. In Fig. 5(b), the solutions corresponding to these trajectories are presented, expressed in terms of the wave variable ξ. (c) Hamiltonian plot of Eq. (3.2). The phase portrait of the two-dimensional system (3.1) is plotted with the parameter values $\omega - 2\alpha > 0, \omega < 0$ for ($\alpha = -3, \beta = 2, \omega = -1$). Fig. 5(a) illustrates the paths followed by the system, showcasing isoclines and nullclines. In Fig. 5(b), the solutions corresponding to these trajectories are presented, expressed in terms of the wave variable ξ. Fig. 5(c) shows the Hamiltonian plot of Eq. (3.2).

Table 1
Comparison of our results with previous results of Mannaf et al. in [48].

Feature	Attain solution of M.A. Mannaf et al.[48]	Obtained solution in this work
Solution	For $\alpha = -1, \beta = 1, \sigma = 1$ we get the solution (3.10) as $V_{1_{12}}(x,t) = -2\tanh\xi$	For $\alpha = 2, \beta = 3, \omega = 3$ we get the solution (4.5) as $V_{3_{12}} = \tanh\frac{1}{\sqrt{6}}\xi$
Soliton type	Standard hyperbolic form	Standard hyperbolic and Trigonometric form
Soliton types	Bright wave, Dark wave, King wave, etc	kink waves, asymmetric periodic waves, and symmetric waves, etc

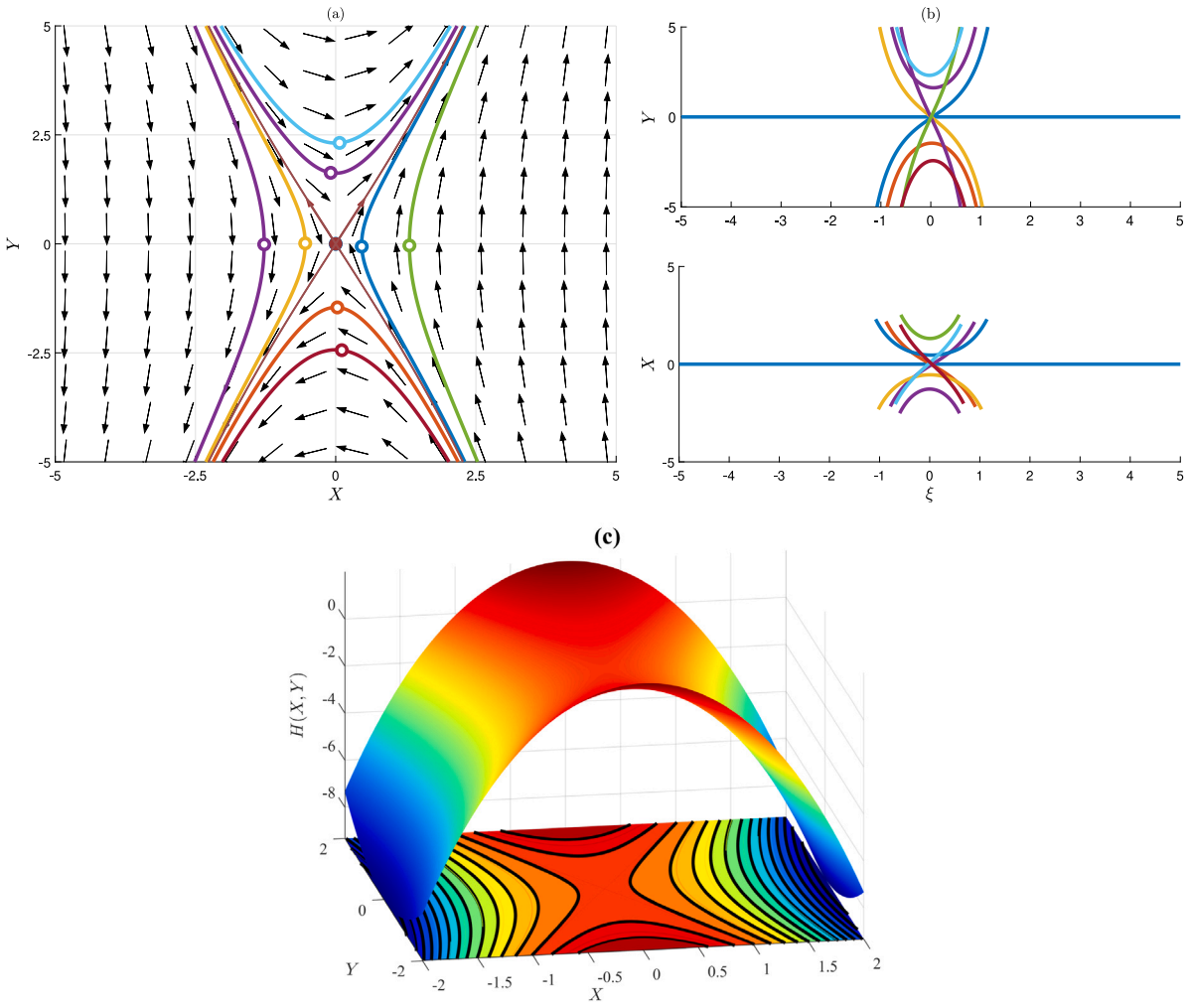

Fig. 6. The phase portrait of the two-dimensional system (3.1) is plotted with the parameter values $\omega - 2\alpha > 0, \omega > 0$ for $(\alpha = -3, \omega = 2, \beta = 2)$. Fig. 6(a) illustrates the paths followed by the system, showcasing isoclines and nullclines. In Fig. 6(b), the solutions corresponding to these trajectories are presented, expressed in terms of the wave variable ξ. Fig. 6(c) displays the Hamiltonian plot of Eq. (3.2).

In summary, the main contributions of this study are threefold: (i) the discovery of a broader family of exact solutions of the SMCH model, including trigonometric, kink-type, and symmetric solitons, beyond those reported in earlier works; (ii) the application of bifurcation analysis and phase portrait methods to the SMCH framework for the first time, providing new insights into the effects of friction and wind parameters on stability and wave dynamics; and (iii) the establishment of an energy-based approach that enhances the interpretability of soliton behavior. Together, these contributions significantly advance the analytical understanding of the SMCH equation and open new avenues for applying nonlinear wave models to realistic physical systems.

7. Conclusion

The SMCH equation has been widely employed to explore different types of water wave phenomena, including solitary waves, wave discontinuities, large-scale ocean disturbances, wind-driven surface waves, and other dynamic wave behaviors. Within this equation, the wind influence parameter α and friction parameter β play pivotal roles in determining wave behavior. Specifically, α dictates the degree of nonlinearity, while β governs dissipation. In practical scenarios, α and β serve as effective tools for modeling diverse wave phenomena. For example, α can represent the influence of wind on water waves, with stronger winds yielding higher waves. Conversely, β captures the impact of friction on wave dynamics, with higher values of β resulting in diminished wave heights due to increased frictional effects.

In this study, we elucidate how α and β correspond to real-world wave phenomena:

- **Wind Influence indicated by α in the SMCH Equation:** Wind blowing over a water surface generates waves, with the wind's strength directly impacting wave height. The SMCH equation incorporates the parameter α to model this wind influence. Higher values of α correspond to stronger wind, leading to the formation of larger waves within the model. By analyzing the obtained wave profile we can state that the model has allowed any value for the parameter α. Besides, the wave shape changes their nature such as stable and unstable waves depending on the value of the parameter where α is negative, positive, or zero.
- **Friction Damping Modeled by β in the SMCH Equation:** Water waves lose energy from friction as they propagate. This friction can arise from various factors, including interaction with the seabed and internal water viscosity. The SMCH equation incorporates the parameter β to model this frictional effect. Higher values of β represent greater friction, leading to the prediction of lower wave heights within the model. By checking the results

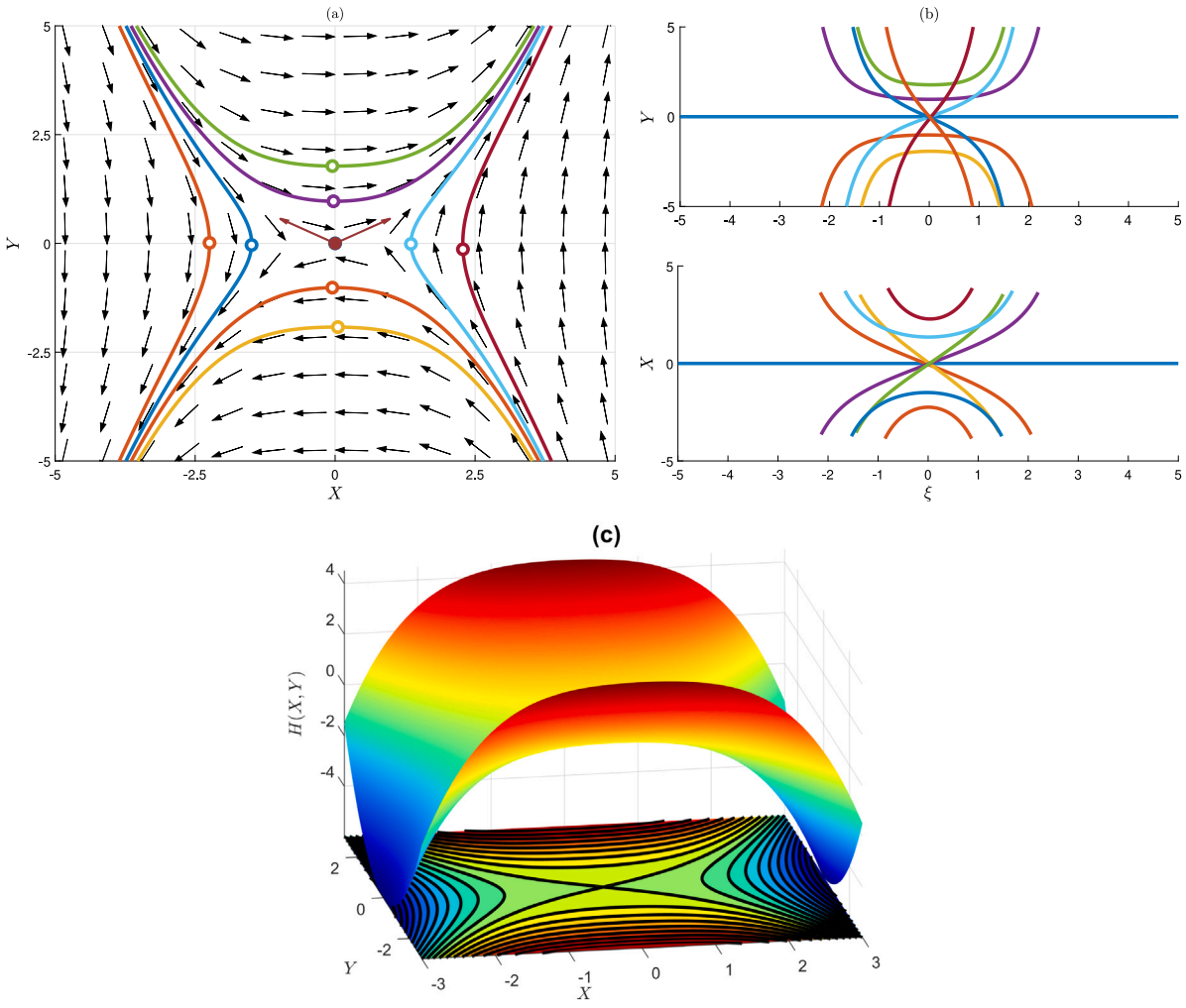

Fig. 7. The phase portrait of the two-dimensional system (3.1) is plotted with the parameter values $\omega - 2\alpha > 0, \omega < 0$ for $(\alpha = 1, \beta = 2, \omega = 3)$. Fig. 7(a) illustrates the paths followed by the system, showcasing isoclines and nullclines. In Fig. 7(b), the solutions corresponding to these trajectories are presented, expressed in terms of the wave variable ξ. Fig. 7(c) displays the Hamiltonian plot of Eq. (3.2).

discussion section we proposed that the parameter β has also impact on the wave profile. For different values of β and freezing the value of other parameters, the same solution represents the different impact on the stability and nature of the waves, those are discussed through the above figures in Section 3.

The SMCH equation plays a crucial role in addressing practical challenges related to wave dynamics. The SMCH equation enables the prediction and analysis of essential wave properties, including height, velocity, and direction. It also allows for the incorporation of variables like wind and friction into wave models, providing valuable insights applicable to diverse areas, including coastal infrastructure development, renewable energy studies, marine science, and environmental protection. It is important to emphasize that, based on the findings of this study, other mathematical models can also contribute significantly to mitigating the impact of natural disasters on the environment.

In addition to solitary wave behavior, the diverse set of solutions obtained in this study — such as kink-type waves and symmetric/asymmetric periodic waves — demonstrates the potential of the SMCH model to describe multi-wave propagation phenomena. These distinct wave profiles can coexist under specific parameter regimes, indicating the model's ability to capture complex nonlinear interactions and the emergence of diverse wave structures.

The derived wave solutions from the SMCH equation have direct and important practical implications. Periodic and kink-type solutions can accurately describe coastal and oceanic wave behaviors under various wind and friction conditions, assisting in the design and optimization of breakwaters, seawalls, and other coastal protection measures. The model's predictive capability can be applied to early-warning systems for extreme wave events and storm surges, improving disaster preparedness. In renewable energy, these solutions offer guidance for the placement and tuning of wave energy converters to maximize harvesting efficiency. Furthermore, by adjusting α and β, the SMCH framework can simulate different climatic and environmental conditions, aiding in climate-change impact studies, environmental forecasting, and sustainable marine resource management. This explicit link between analytic solutions and actionable engineering or environmental strategies bridges the gap between theoretical nonlinear wave analysis and real-world problem solving.

Despite these promising results, this study has some limitations. The analysis is restricted to the one-dimensional SMCH equation under idealized conditions, neglecting effects such as variable water depth, multidimensional interactions, and stochastic environmental influences. Future work could extend the current framework to higher-dimensional models, include additional physical factors, and explore chaotic or turbulent wave regimes to better reflect real-world ocean dynamics.

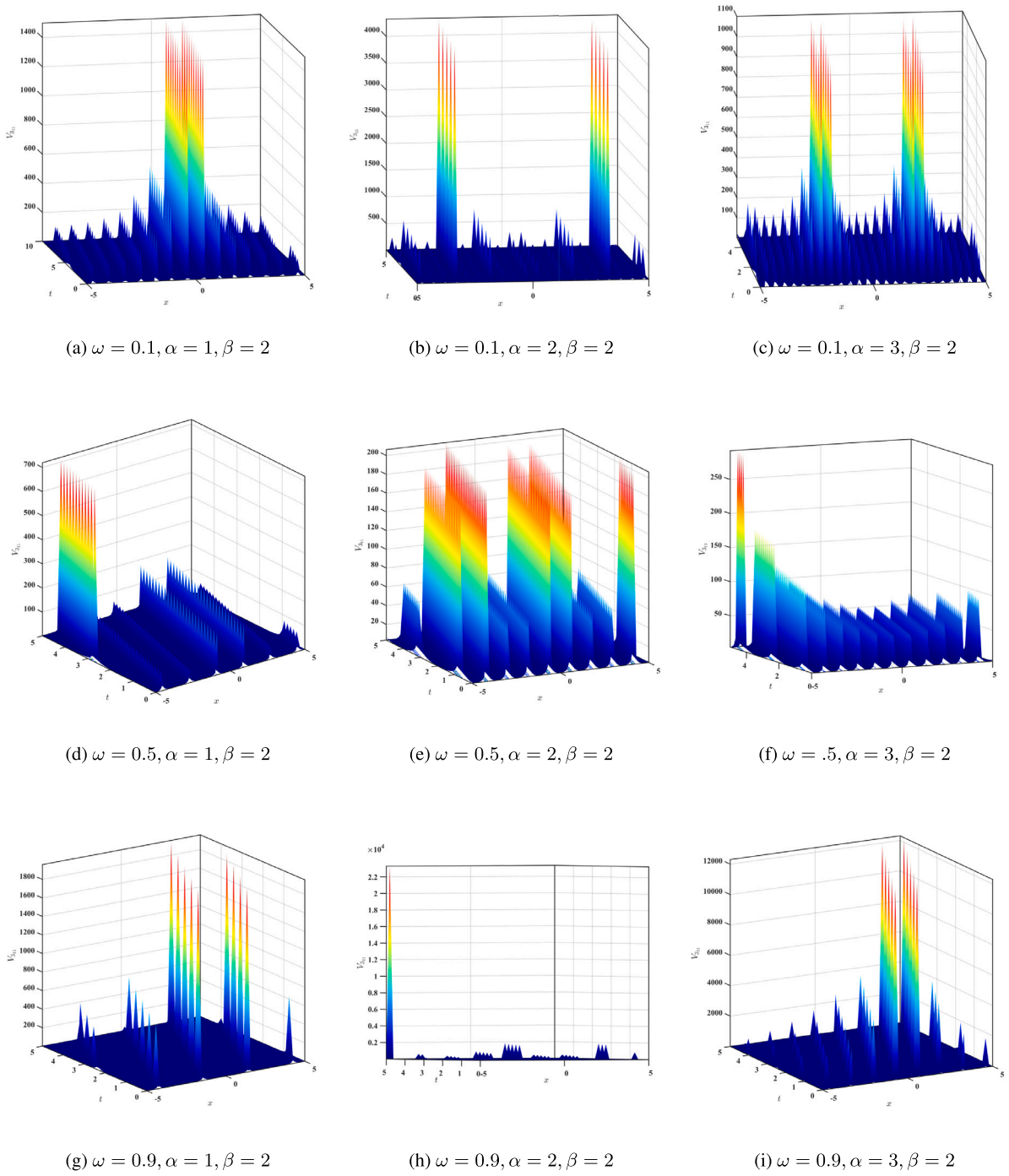

(a) $\omega = 0.1, \alpha = 1, \beta = 2$ (b) $\omega = 0.1, \alpha = 2, \beta = 2$ (c) $\omega = 0.1, \alpha = 3, \beta = 2$

(d) $\omega = 0.5, \alpha = 1, \beta = 2$ (e) $\omega = 0.5, \alpha = 2, \beta = 2$ (f) $\omega = .5, \alpha = 3, \beta = 2$

(g) $\omega = 0.9, \alpha = 1, \beta = 2$ (h) $\omega = 0.9, \alpha = 2, \beta = 2$ (i) $\omega = 0.9, \alpha = 3, \beta = 2$

Fig. 8. The results present a visualization of the solution $V_{3_{11}}$ in the form of three-dimensional plots, illustrating the influence of the velocity parameter ω (rows) and the shape parameter α (columns) on the system response, with the scale parameter fixed at $\beta = 2$. The rows correspond to $\omega = 0.1, 0.5$, and 0.9, while the columns correspond to $\alpha = 1, 2$, and 3.

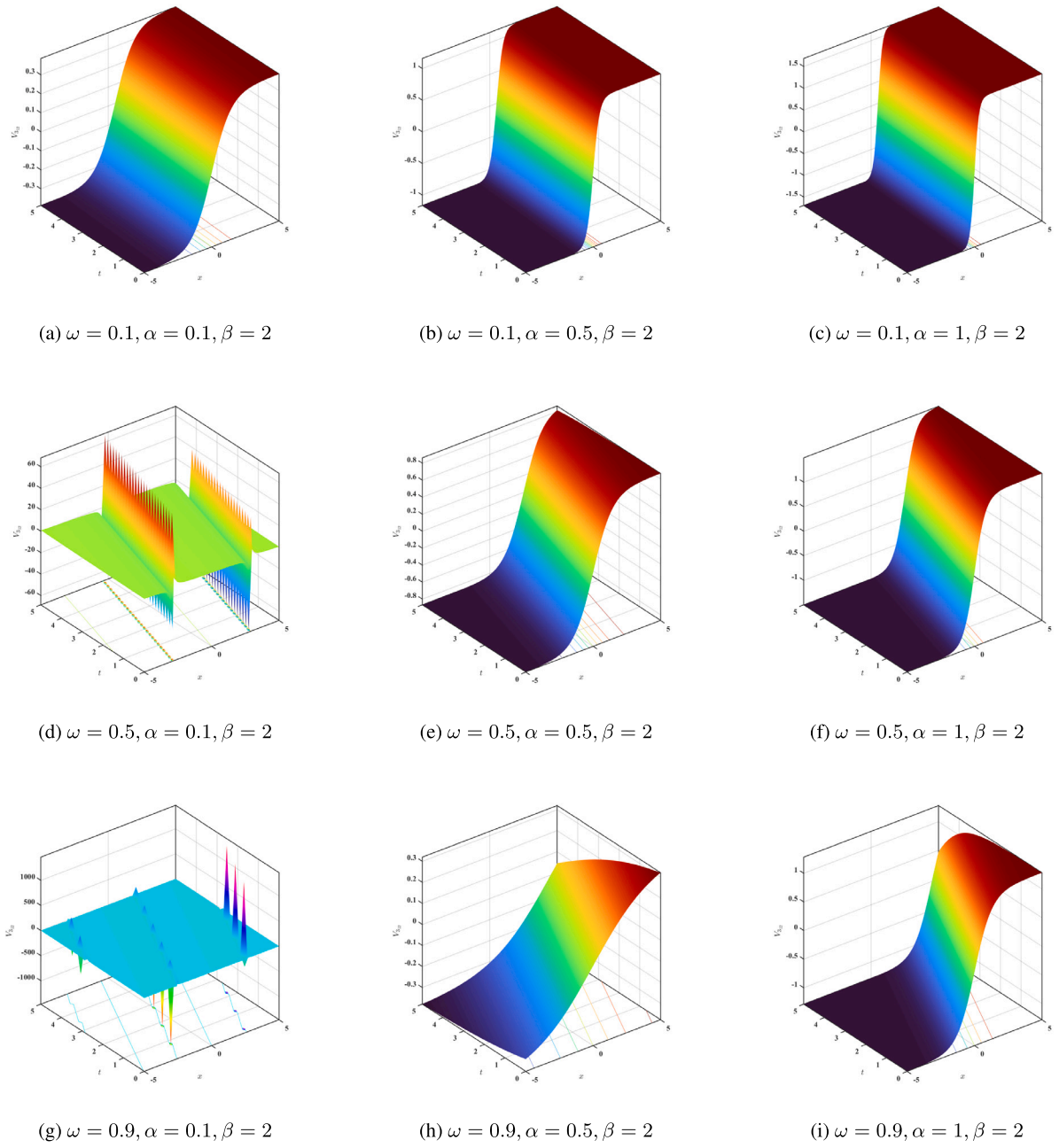

(a) $\omega = 0.1, \alpha = 0.1, \beta = 2$ (b) $\omega = 0.1, \alpha = 0.5, \beta = 2$ (c) $\omega = 0.1, \alpha = 1, \beta = 2$

(d) $\omega = 0.5, \alpha = 0.1, \beta = 2$ (e) $\omega = 0.5, \alpha = 0.5, \beta = 2$ (f) $\omega = 0.5, \alpha = 1, \beta = 2$

(g) $\omega = 0.9, \alpha = 0.1, \beta = 2$ (h) $\omega = 0.9, \alpha = 0.5, \beta = 2$ (i) $\omega = 0.9, \alpha = 1, \beta = 2$

Fig. 9. The results present a visualization of the solution $V_{3_{12}}$ in the form of three-dimensional plots, illustrating the influence of the velocity parameter ω (rows) and the shape parameter α (columns) on the system response, with the scale parameter fixed at $\beta = 2$. The rows correspond to $\omega = 0.1, 0.5$, and 0.9, while the columns correspond to $\alpha = 0.1, 0.5$, and 1.

Funding statement

No funding was received for this research

Declaration of competing interest

The authors declare that they have no known competing financial interests or personal relationships that could have appeared to influence the work reported in this paper.

Acknowledgment

USB gratefully acknowledges the University of Konstanz and the Max Planck Institute of Animal Behavior (MPI-AB) for providing research space and support during his postdoctoral stay, during which this research was conducted.

Data availability

All data generated or analyzed during this study are included in this published article.

References

[1] Md Habibul Bashar, Mustafa Inc, S.M. Rayhanul Islam, K.H. Mahmoud, M. Ali Akbar, Alexandria Eng. J. 61 (12) (2022) 12539–12547.
[2] S.M. Rayhanul Islam, Udoy Sankar Basak, Partial Differ. Equ. Appl. Math. 8 (2023) 100561.
[3] Shao-Wen Yao, Naeem Ullah, Hamood Ur Rehman, Mir Sajjad Hashemi, Mohammad Mirzazadeh, Mustafa Inc, Results Phys. 48 (2023) 106448.
[4] S.M. Rayhanul Islam, Kamruzzaman Khan, K.M. Abdul Al Woadud, Waves Random Complex Media 28 (2) (2018) 300–309.
[5] Md Ekramul Islam, Md Motaleb Hossain, Khalifa Mohammad Helal, Udoy S. Basak, Rajandra Chadra Bhowmik, M.A. Akbar, Arab J. Basic Appl. Sci. 30 (1) (2023) 329–340.
[6] Abdul-Majid Wazwaz, Lakhveer Kaur, Optik 184 (2019) 428–435.
[7] Sudhir Singh, Lakhveer Kaur, R. Sakthivel, K. Murugesan, Physica A 560 (2020) 125114.
[8] Ruijuan Li, Jalil Manafian, Holya A. Lafta, Hawraa A. Kareem, Khusnidin Fakhriddinovich Uktamov, Mostafa Abotaleb, Int. J. Geom. Methods Mod. Phys. 19 (10) (2022) 2250151.
[9] Qingchen Lu, Onur Alp Ilhan, Jalil Manafian, Laleh Avazpour, Int. J. Comput. Math. 98 (7) (2021) 1457–1473.
[10] Jalil Manafian, Onur Alp Ilhan, Hajar Farhan Ismael, Sizar Abid Mohammed, Saadat Mazanova, Int. J. Comput. Math. 98 (8) (2021) 1594–1616.
[11] Kamruzzaman Khan, M. Ali Akbar, Ain Shams Eng. J. 4 (4) (2013) 903–909.
[12] Emrullah Yaşar, Yakup Yıldırım, Qin Zhou, Seithuti P. Moshokoa, Malik Zaka Ullah, Houria Triki, Anjan Biswas, Milivoj Belic, Superlattices Microstruct. 111 (2017) 487–498.
[13] Mohammad Mirzazadeh, Mostafa Eslami, Essaid Zerrad, Mohammad F. Mahmood, Anjan Biswas, Milivoj Belic, Nonlinear Dynam. 81 (2015) 1933–1949.
[14] Wen-Xiu Ma, Phys. Lett. A 379 (36) (2015) 1975–1978.
[15] Arifa Mirza, Mahmood ul Hassan, J. Nonlinear Math. Phys. 24 (1) (2017) 107–115.
[16] Wei-Ping Zhong, Milivoj Belić, Gaetano Assanto, Boris A. Malomed, Tingwen Huang, Phys. Rev. A 84 (4) (2011) 043801.
[17] Wei-Ping Zhong, Milivoj R. Belić, Gaetano Assanto, Boris A. Malomed, Tingwen Huang, Phys. Rev. A 83 (4) (2011) 043833.
[18] Mohammad Safi Ullah, Partial Differ. Equ. Appl. Math. 8 (2023) 100566.
[19] Yingfang Pan, Jalil Manafian, Subhiya M. Zeynalli, Riyadh Al-Obaidi, R. Sivaraman, Ammar Kadi, Qual. Theory Dyn. Syst. 21 (4) (2022) 127.
[20] Md Abde Mannaf, Md Ekramul Islam, Habibul Bashar, Udoy Sankar Basak, M. Ali Akbar, Results Phys. 57 (2024) 107324.
[21] Slobodan Zdravković, Louis Kavitha, Miljko V. Satarić, Slobodan Zeković, Jovana Petrović, Chaos Solitons Fractals 45 (11) (2012) 1378–1386.
[22] Md Sabur Uddin, Momtaz Begum, Mohammad Safi Ullah, Alrazi Abdeljabbar, et al., Partial Differ. Equ. Appl. Math. 8 (2023) 100591.
[23] Md Abde Mannaf, Rajandra Chadra Bhowmik, Mst Tania Khatun, Md Ekramul Islam, Udoy S. Basak, M. Ali Akbar, Partial Differ. Equ. Appl. Math. 8 (2023) 100588.
[24] Abdul Hamid Ganie, Abdul-Majid Wazwaz, Aly R. Seadawy, Mohammad Safi Ullah, Humayra Dil Afroz, Rabeya Akter, Pramana 98 (2) (2024) 46.
[25] Ji-Huan He, Xu-Hong Wu, Chaos Solitons Fractals 30 (3) (2006) 700–708.
[26] Yuanlin Liu, Zhimin Ma, Ruoyang Lei, Nonlinear Dynam. 112 (4) (2024) 2837–2849.
[27] Wen-Xiu Ma, Chaos Solitons Fractals 146 (2021) 110824.
[28] Nauman Raza, Melike Kaplan, Ahmad Javid, Mustafa Inc, Opt. Quantum Electron. 54 (2022) 1–16.
[29] Adil Jhangeer, Beenish, Abdallah M. Talafha, Ali R. Ansari, Mudassar Imran, Arab J. Basic Appl. Sci. 31 (1) (2024) 536–553.
[30] Ahmad Javid, Aly R. Seadawy, Nauman Raza, Phys. Lett. A 407 (2021) 127446.
[31] Wen-Xiu Ma, Jyh-Hao Lee, Chaos Solitons Fractals 42 (3) (2009) 1356–1363.
[32] Wen-Xiu Ma, Axioms 13 (7) (2024) 481.
[33] M. Ali Akbar, Norhashidah Hj Mohd Ali, Cogent Math. 4 (1) (2017) 1282577.
[34] Wen-Xiu Ma, Theoret. and Math. Phys. 221 (1) (2024) 1603–1614.
[35] Mahmoud A.E. Abdelrahman, Emad H.M. Zahran, Mostafa M.A. Khater, et al., Int. J. Modern Nonlinear Theory Appl. 4 (01) (2015) 37.
[36] Zhi-Min Ma, Yu-Huai Sun, Fu-Sheng Liu, Commun. Theor. Phys. (Beijing) 59 (3) (2013) 307.
[37] Tarikul Islam, M. Ali Akbar, Abul Kalam Azad, J. Ocean Eng. Sci. 3 (1) (2018) 76–81.
[38] Zhimin Ma, Binji Wang, Xukun Liu, Yuanlin Liu, Pramana 98 (1) (2024) 1–13.
[39] Jie Zhong, Zhimin Ma, Binji Wang, Yuanlin Liu, Internat. J. Theoret. Phys. 62 (12) (2023) 268.
[40] Nauman Raza, Muhammad Abdullah, Asma Rashid Butt, Isma Ghulam Murtaza, Sultan Sial, Opt. Quantum Electron. 50 (2018) 1–17.
[41] Nauman Raza, Adil Jhangeer, Zeeshan Amjad, Beenish Rani, Taseer Muhammad, Nonlinear Dynam. 112 (24) (2024) 22323–22341.
[42] Adil Jhangeer, Haiqa Ehsan, Muhammad Bilal Riaz, Abdallah M. Talafha, Partial Differ. Equ. Appl. Math. 12 (2024) 100966.
[43] Roberto Camassa, Darryl D. Holm, Phys. Rev. Lett. 71 (11) (1993) 1661.
[44] Tifei Qian, Minying Tang, Chaos Solitons Fractals 12 (7) (2001) 1347–1360.
[45] Abdul-Majid Wazwaz, Appl. Math. Comput. 163 (3) (2005) 1165–1179.
[46] Jianwei Shen, Wei Xu, Chaos Solitons Fractals 26 (4) (2005) 1149–1162.
[47] Amna Irshad, Muhammad Usman, Syed Tauseef Mohyud-Din, Int. J. Modern Math. Sci. 4 (3) (2012) 146–155.
[48] Md Abde Mannaf, Rajandra Chadra Bhowmik, Mst Tania Khatun, Md Ekramul Islam, Udoy S. Basak, M. Ali Akbar, Opt. Quantum Electron. 56 (1) (2024) 71.
[49] Malihe Najafi, Somayeh Arbabi, Mohammad Najafi, Int. J. Phys. Res. 1 (2013) 1–6.
[50] Md Nur Alam, M. Ali Akbar, J. Assoc. Arab Univ. Basic Appl. Sci. 17 (2015) 6–13.
[51] Hasibun Naher, Fardousi Ara Begum, Amer. J. Appl. Math. Stat. 3 (1) (2015) 23–28.
[52] Ayyaz Ali, Muhammad Asad Iqbal, Syed Tauseef Mohyud-Din, Egypt. J. Basic Appl. Sci. 3 (2) (2016) 134–140.
[53] Dianchen Lu, Aly R. Seadawy, Mujahid Iqbal, Open Phys. 16 (1) (2018) 896–909.
[54] Md Nurul Islam, Md Asaduzzaman, Md Shajib Ali, AIMS Math. 5 (1) (2019) 26–41.
[55] S.M. Rayhanul Islam, S.M. Yiasir Arafat, Hanfeng Wang, J. Ocean Eng. Sci. (2022).
[56] Syeda Sarwat Kazmi, Adil Jhangeer, Nauman Raza, Haifa I. Alrebdi, Abdel-Haleem Abdel-Aty, Hichem Eleuch, Symmetry 15 (7) (2023) 1324.
[57] Barka Infal, Adil Jhangeer, Muhammad Muddassar, Int. J. Geom. Methods Mod. Phys. 22 (05) (2025) 2450320.
[58] S.M. Rayhanul Islam, S.M. Yiasir Arafat, Hanfeng Wang, J. Ocean Eng. Sci. 8 (3) (2023) 238–245.